Vietnam Journal of Mechanics, Vol. 48, No. 2 (2026), pp. 105 – 119
DOI: https://doi.org/10.15625/0866-7136/23425

A PHASE FIELD - UEL FRAMEWORK FOR CRACK BRANCHING SIMULATION IN CONCRETE

Vu Thi Thuy Anh[*], **Ha Chi Hieu, Phan Dang Huy**
Faculty of Civil Engineering, VNU University of Engineering and Technology,
144 Xuan Thuy Street, Cau Giay Ward, Hanoi, Vietnam
[*]E-mail: anhvutt@vnu.edu.vn

Received: 17 September 2025 / Revised: 23 October 2025 / Accepted: 29 October 2025
Published online: 9 June 2026

Abstract. Crack branching significantly affects the fracture behavior of concrete, yet its modeling remains challenging due to the quasi-brittle nature of the material. This study presents an implementation of the Phase Field Method (PFM) within Abaqus using a User Element (UEL) subroutine to simulate the initiation and propagation of cracks in pre-notched concrete plates. The proposed framework enables a continuous description of fracture without explicit crack surface tracking, thus providing numerical stability when complex branching occurs. Through a series of simulations, the influence of material properties, loading configurations, and mesh resolution on crack evolution is examined. The findings demonstrate that the PFM–UEL framework can effectively capture branching patterns and deliver consistent fracture responses, thereby underscoring its potential as a robust tool for analyzing concrete failure and supporting future data-driven modeling efforts.

Keywords: crack branching, crack propagation, phase field, UEL, ABAQUS.

1. INTRODUCTION

When cracks occur in concrete structures, their initiation and subsequent propagation are primarily driven by the underlying stress field. Unlike idealized flaws often assumed in theoretical models, cracks in concrete are highly irregular in both geometry and size due to the heterogeneous composition of the material. For classification purposes (Fig. 1), they are commonly grouped into single cracks (a), branched cracks (b), and complex crack networks (c). In practice, however, cracks rarely remain as isolated entities; once initiated, they tend to evolve into branched or interconnected networks. Such fracture patterns have a profound impact on the residual load-carrying capacity, durability, and overall service life of structures. Despite this practical importance, the majority of existing research both internationally and in Vietnam has focused mainly on single cracks, which limits the ability of current approaches to fully capture the intricate fracture processes observed in real concrete structures.

Over the past decades, several fracture mechanics frameworks have been established to describe the initiation and propagation of cracks, most notably Linear Elastic Fracture Mechanics (LEFM), Nonlinear Fracture Mechanics (NLFM), the Cohesive Zone Model (CZM), and Continuum Damage Mechanics (CDM). LEFM provides a rigorous mathematical foundation but is restricted to linear elastic behavior. NLFM overcomes this limitation by incorporating nonlinear effects, while CZM introduces traction–separation relations that allow crack initiation without stress singularities. CDM, in contrast, represents material degradation continuously through internal variables. Together, these models have advanced understanding of fracture,

yet they remain formulated under idealized conditions and are not fully capable of representing the heterogeneous, quasi-brittle behavior of concrete, which is highly sensitive to loading and environmental factors.

To address these limitations, advanced numerical methods have been developed. The Finite Element Method (FEM) is widely used but is hampered by costly re-meshing when simulating crack propagation (C. Wang et al., 2023). The Extended Finite Element Method (XFEM) improves efficiency by enriching displacement fields, yet it still struggles with spontaneous branching (L.-X. Wang et al., 2024). Peridynamics (PD) offers a nonlocal formulation that naturally captures initiation and branching but at a substantial computational cost (Dorduncu et al., 2024). More recently, the PFM has emerged as a powerful alternative. By describing cracks as a continuous damage field derived from an energy minimization principle, PFM enables stable simulations of nucleation, branching, and complex crack networks without explicit crack tracking, although the approach still demands significant computational resources (Azinpour et al., 2023; Nair & Ghosh, 2023; Zhang et al., 2025).

(a) Single crack (b) Branching crack (c) Complex cracks

Fig. 1. Classification of concrete cracks

For single crack problems, the XFEM is often the method of choice because of its lower computational cost and efficiency in handling relatively simple crack paths. However, when branching phenomena occur, XFEM encounters difficulties in accurately tracking multiple evolving fronts. In contrast, the PFM offers distinct advantages. By smearing cracks as a continuous field, it allows adaptive refinement of the mesh along the evolving crack paths, which significantly improves the reliability of predicting ultimate loads and capturing the transition from a single crack to multiple branches (Abdulridha Lateef et al., 2022). A number of comparative studies have confirmed that PFM generally yields more stable and robust results than XFEM when simulating crack branching and complex crack networks (Abdulridha Lateef et al., 2022; Khan et al., 2023; Li & Xu, 2022). Despite these strengths, most existing works are still confined to relatively simple benchmark problems and small-scale models. They often rely on academic platforms such as MATLAB or FreeFEM for implementation, and systematic efforts to exploit PFM as a basis for large-scale dataset generation, particularly for machine learning (ML) or deep learning (DL) applications, are still lacking.

In Vietnam, research that combines theoretical analysis, numerical simulation, and experimental validation has become increasingly prominent in recent years. Representative contributions can be found in the works of Hang (2015) and Khiem and Hang (2017), Huong (2016) and Huong et al. (2015), Chung et al. (2016), and Truong et al. (2021), as well as the group of Duc et al. (2018) and Minh et al. (2018). These studies have enriched the domestic research landscape, yet most remain centered on structural systems with pre-existing cracks. The predominant approaches involve vibration-based analyses, meshfree formulations, or standalone applications of PFM, thereby addressing mainly stationary crack scenarios rather than modeling the full crack propagation process.

More recently, Anh et al. (2025) and Dinh et al. (2023) have taken a step forward by integrating fracture mechanics, XFEM, and machine learning (ML) to generate large-scale numerical

datasets. This line of work has proven cost-effective compared with experimental testing and has shown strong correlation with observed cracking patterns, demonstrating the feasibility of data-driven fracture analysis. Nevertheless, the limitation lies in its scope: the datasets are restricted to single-crack cases, which inevitably diminishes the predictive accuracy of ML models when confronted with branched or complex crack networks (Fig. 2; (Anh et al., 2025)). These shortcomings underline the need for extended research frameworks capable of capturing branching phenomena and of providing richer datasets to enhance the generalization capabilities of ML/DL models.

As highlighted above, the PFM is particularly well suited for modeling crack branching because it captures complex fracture patterns within a unified theoretical framework. However, its application to structural-scale concrete analysis remains relatively limited. Previous attempts to integrate PFM into commercial finite element platforms, such as Abaqus, have often relied on UEL subroutines (Molnár et al., 2020; Navidtehrani et al., 2021a, 2021b; Yu et al., 2023). While these implementations demonstrate the feasibility of embedding phase-field formulations into general-purpose solvers, most studies have concentrated on brittle materials such as ceramics, glass, or metals (Reddy et al., 2021; Sun et al., 2021; Zhou et al., 2023), and have typically focused only on single-crack propagation.

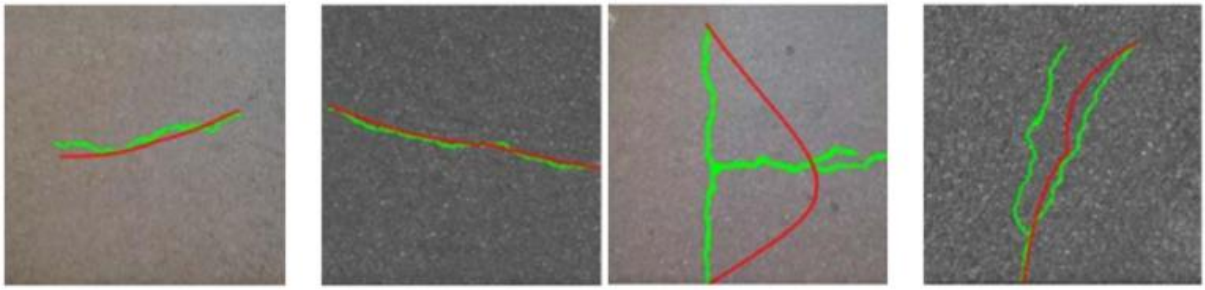

Fig. 2. Correlation between the prediction model based on single-crack datasets and real crack patterns (Anh et al., 2025)

For concrete, a quasi-brittle material in which the fracture process zone (FPZ) strongly governs crack initiation, propagation, and eventual branching, the use of PFM remains limited. Existing works are often confined to microscale analyses or highly idealized 3D models (Hai et al., 2024; Li & Xu, 2022). Such models, although valuable, are not easily scalable to structural applications and are insufficient for generating comprehensive datasets that could be leveraged for advanced machine learning tasks.

To overcome these limitations, the present study introduces a dedicated UEL framework that embeds the PFM into Abaqus specifically for quasi-brittle materials. This framework enables the consistent simulation of both single and branched cracks in concrete, extending the scope of phase-field modeling from benchmark problems to more realistic structural applications. While the present study focuses on representative single and branched crack scenarios, the framework is inherently scalable to larger-scale structural applications, providing a foundation for future investigations. Unlike previous PFM-UEL implementations that focus mainly on brittle materials or single-crack propagation, the present framework addresses quasi-brittle concrete, supports both single and branched cracks, and provides a robust basis for automated dataset generation to facilitate ML-based crack analysis.

2. PHASE FIELD METHODOLOGY AND UEL BASED NUMERICAL FRAMEWORK

Modeling crack propagation in concrete is particularly challenging due to its heterogeneous microstructure and the complex fracture patterns such as branching. Classical discrete

approaches require explicit tracking of evolving crack surfaces, which is computationally demanding and prone to numerical instabilities. The PFM provides a powerful alternative by introducing a continuous scalar variable $\phi \in [0,1]$ that smoothly represents the crack state, with $\phi = 0$ denoting the intact material and $\phi = 1$ denoting the fully broken state. In quasi-brittle materials such as concrete, the elastic strain energy is decomposed spectrally into tensile and compressive parts, where only the tensile contribution is degraded. This prevents spurious crack growth under compression and ensures realistic fracture patterns.

The total energy functional in the PFM is therefore defined as the sum of the degraded tensile strain energy, the intact compressive strain energy, and the fracture energy contribution, minus the external work. This represents the balance between elastic energy, fracture energy, and external work, forming the variational foundation of the phase-field fracture model (Bažant & Planas, 1998; Miehe et al., 2010):

$$\Psi(\mathbf{u},\phi) = \int_\Omega \left(g(\phi)\psi^+(\varepsilon(\mathbf{u})) + \psi^-(\varepsilon(\mathbf{u}))\right) \mathrm{d}V + \int_\Omega G_c \gamma(\phi,\nabla\phi)\mathrm{d}V - \int_\Omega \mathbf{b}\cdot\mathbf{u}\,\mathrm{d}V - \int_{\partial\Omega_t} \bar{\mathbf{t}}\cdot\mathbf{u}\,\mathrm{d}S, \tag{1}$$

where $g(\phi) = (1-\phi)^2 + k$ is a degradation function, $k \ll 1$ is a small stabilization parameter; ψ^+, ψ^- are the tensile and compressive parts of the elastic strain energy density; G_c the critical fracture energy; and $\gamma(\phi,\nabla\phi) = \dfrac{\phi^2}{2\ell} + \dfrac{\ell}{2}|\nabla\phi|^2$ is the crack surface density function with length-scale parameter ℓ. The displacement field is $\mathbf{u}$, with the strain tensor $\varepsilon(\mathbf{u}) = \dfrac{1}{2}\left(\nabla\mathbf{u} + \nabla\mathbf{u}^T\right)$.

An important distinction arises when modeling single crack propagation versus crack branching in the phase-field framework. For single cracks, the phase-field variable ϕ evolves smoothly along a unique energy-minimizing path, which is often aligned with the maximum principal stress direction. In contrast, branching occurs when stress redistribution at the crack tip activates multiple competing paths, leading to several local minima of the total energy functional. The diffusive representation of ϕ naturally captures such bifurcations without the need for pre-imposed branching criteria, remeshing, or explicit tracking of crack surfaces. This capability makes the PFM particularly appealing for quasi-brittle materials such as concrete, where branching and multiple crack interactions are commonly observed. In practice, the accuracy of this formulation depends on the calibration of fracture energy G_c and the length-scale parameter ℓ, which together govern energy dissipation and the width of the diffused crack zone. These parameters are typically determined through experimental tests or inverse modeling.

The governing equations are derived from the variational principle by taking variations of the total energy functional with respect to the displacement field $\mathbf{u}$ and the crack phase-field ϕ. The coupled system includes the mechanical equilibrium equation and the phase-field evolution equation (Miehe et al., 2010):

$$\nabla\cdot\boldsymbol{\sigma} + \mathbf{b} = 0, \quad \boldsymbol{\sigma} = g(\phi)\mathbf{C} : \varepsilon(\mathbf{u}), \quad G_c\left(\frac{\phi}{\ell} - \ell\Delta\phi\right) - 2(1-\phi)H = 0, \tag{2}$$

here, $H(\mathbf{x},t) = \max\limits_{s\le t} \psi^+(\varepsilon(\mathbf{u}(\mathbf{x},s)))$ is the history field storing the maximum tensile energy, ensuring irreversibility of fracture (ϕ cannot decrease).

By taking variations of the total energy functional with respect to the displacement field $\mathbf{u}$ and the crack phase-field ϕ, the weak forms of the governing equations are obtained. The weak form of the mechanical equilibrium equation reads:

$$\int_\Omega \boldsymbol{\sigma} : \delta\varepsilon\,\mathrm{d}V - \int_\Omega \delta\mathbf{u}\cdot\mathbf{b}\,\mathrm{d}V - \int_{\partial\Omega_t} \delta\mathbf{u}\cdot\bar{\mathbf{t}}\,\mathrm{d}S = 0, \tag{3}$$

where $\delta\mathbf{u}$ is the virtual displacement, $\mathbf{b}$ the body force vector, and $\bar{\mathbf{t}}$ the prescribed traction. Similarly, the weak form of the phase-field equation is given by

$$\int_{\Omega} \left[G_c \left(\frac{\phi}{\ell}\eta + \ell \nabla\phi \cdot \nabla\eta \right) - 2(1-\phi)H\eta \right] \mathrm{d}V = 0, \tag{4}$$

with η denotes the test function associated with the scalar field ϕ.

After finite element discretization, the coupled residual system can be expressed as

$$\mathbf{R}_u = \mathbf{f}_{int} - \mathbf{F}_{ext} = 0, \quad \mathbf{R}_\phi = 0, \tag{5}$$

where $\mathbf{R}_u$ corresponds to the vector of mechanical equilibrium residuals and $\mathbf{R}_\phi$ is the scalar residual associated with the phase-field equation. $\mathbf{f}_{int}$ denotes the internal force vector obtained from the stress field, while $\mathbf{F}_{ext}$ represents the external force vector from body forces and tractions. The residual form $\mathbf{R}_u = \mathbf{f}_{int} - \mathbf{F}_{ext}$ enforces the balance between internal and external forces.

For practical implementation within the finite element framework, the present phase-field formulation is embedded into ABAQUS through a UEL. Several considerations are necessary to ensure numerical robustness. To prevent spurious crack growth under compression, the strain energy density is decomposed spectrally, degrading only the tensile contribution. The internal length scale ℓ governs the width of the diffused crack band, requiring a sufficiently refined mesh (typically $h \leq \ell/2$ or $h \leq \ell/3$) to maintain mesh objectivity. A small stabilization parameter $k \in \left[10^{-8}, 10^{-6}\right]$ is introduced to avoid singularities as $\phi \to 1$, while remaining small enough not to affect fracture behavior. With respect to crack nucleation and propagation, different formulations either provide a sharp initiation threshold or a smooth degradation law; the latter is more commonly adopted in UEL-based simulations of branching cracks due to its numerical stability.

Crack branching itself emerges naturally from the phase-field representation; nevertheless, in practice, incremental loading combined with small perturbations (e.g., from geometric or material asymmetry) is applied to promote consistent path selection. With these considerations, the theoretical formulation provides a consistent foundation for UEL implementation in ABAQUS.

The weak forms of the displacement and phase-field equations provide natural element-level residuals and tangent operators that can be directly implemented in ABAQUS via a UEL. Using UEL permits defining custom degrees of freedom (DOFs) per node (e.g. displacement components and the scalar phase-field), assembling element residuals and consistent tangents, and thus solving the coupled fracture problem within ABAQUS's Newton–Raphson solver.

Interpolate displacement and phase-field at element level (discretization and element variables):

$$\mathbf{u}(x) \approx \mathbf{N}_u(x)\mathbf{u}_e, \quad \phi(x) \approx N_\phi(x)\phi_e, \tag{6}$$

here $\mathbf{N}_u(x)$ is the vector/block shape-function matrix for vector displacements and N_ϕ for scalar phase field. (In practice both fields can use the same interpolation order; linear elements are common, but quadratic may improve accuracy), and $\varepsilon = \mathbf{B}\mathbf{u}_e$ with standard strain displacement $\mathbf{B}$ matrix.

At each element, Gauss quadrature evaluates element contributions and updates Gauss-point variables (notably the history field H). The element residual vectors are

$$\begin{aligned} \mathbf{R}_{u,e} &= \int_{\Omega_e} \mathbf{B}^T \boldsymbol{\sigma}\, \mathrm{d}V - \int_{\Omega_e} \mathbf{N}_u^T \mathbf{b}\, \mathrm{d}V - \int_{\partial\Omega_{t,e}} \mathbf{N}_u^T \bar{\mathbf{t}}\, \mathrm{d}S, \\ \mathbf{R}_{\phi,e} &= \int_{\Omega_e} \left[G_c \left(\frac{\phi}{\ell} N_\phi + \ell \nabla\phi \cdot \nabla N_\phi \right) - 2(1-\phi)H N_\phi \right] \mathrm{d}V, \end{aligned} \tag{7}$$

with $\boldsymbol{\sigma}$ is evaluated using the constitutive split defined above (e.g. $\boldsymbol{\sigma} = g(\phi)\dfrac{\partial \psi^+}{\partial \varepsilon} + \dfrac{\partial \psi^-}{\partial \varepsilon}$ if spectral split is used). Note that $\mathbf{R}_{\phi,e}$ above is written in a form convenient for numerical integration (the gradient term is implemented by computing $\nabla\phi$ from nodal ϕ_e and contracting with ∇N_ϕ).

For a Newton–Raphson solution the consistent element tangent is assembled in block form:

$$\mathbf{K}_e = \begin{bmatrix} \mathbf{K}_{uu} & \mathbf{K}_{u\phi} \\ \mathbf{K}_{\phi u} & \mathbf{K}_{\phi\phi} \end{bmatrix}, \tag{8}$$

For Newton–Raphson solution the consistent element tangent matrix is assembled in block form $\mathbf{K}_e$. In practice, the spectral split of the strain energy, Gauss-point storage of the history field H, sufficient mesh refinement relative to ℓ, and careful linearization of split terms are essential for robustness. Implementation may follow either a staggered solution scheme (simpler) or a fully coupled monolithic scheme (higher performance but more complex) (Tanné et al., 2018).

The UEL returns element residuals (and tangents if available) to ABAQUS for global assembly; the global Newton solver then updates nodal $\mathbf{u}$ and ϕ and iterates until convergence. To illustrate the computational workflow, the following block diagram summarizes the key steps of the UEL implementation, from field interpolation to the integration with ABAQUS.

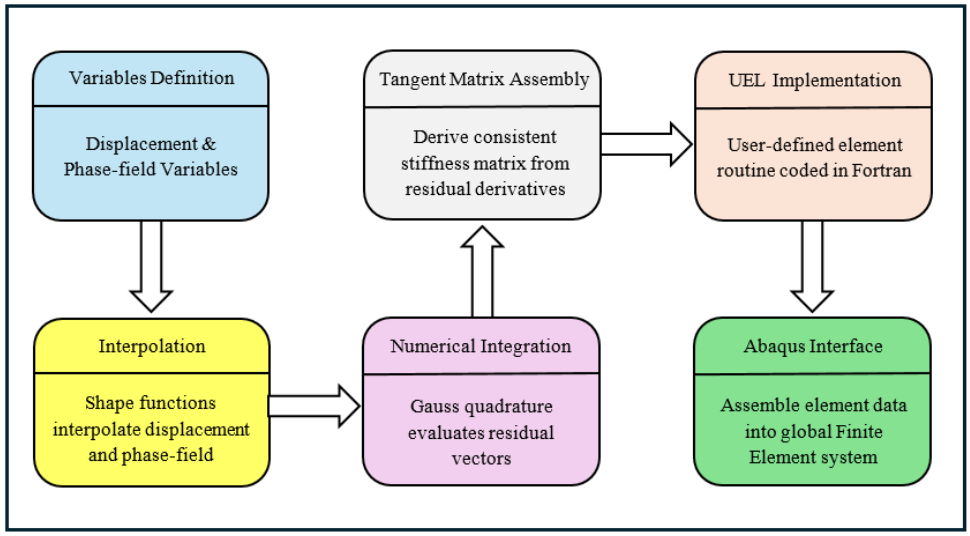

Fig. 3. Block diagram of the PFM – UEL framework implemented in ABAQUS for simulating crack branching in concrete

In this framework, the phase-field variable ϕ is explicitly introduced as an additional nodal degree of freedom within each UEL, alongside the standard displacement DOFs. The element residual and Jacobian contributions for both displacement and ϕ are assembled into the global system by Abaqus. A staggered implicit scheme is adopted: at each increment, Abaqus first solves the mechanical equilibrium problem, and then the UEL updates ϕ using the stored history field, which ensures irreversibility of damage. This formulation allows Abaqus to control the global solution process (Newton–Raphson iterations, load stepping, and convergence checks), while the UEL governs the evolution law and consistency of the phase-field variable at the element level. As a result, the PFM–UEL framework provides a transparent yet flexible coupling, capable of reproducing both single and branching crack propagation in quasi-brittle materials.

The theoretical foundations of the phase-field method and its UEL implementation in ABAQUS establish a consistent framework for simulating both single and branching cracks in concrete. Building on this framework, the following section presents its application to specific benchmark problems to demonstrate accuracy and robustness.

3. APPLICATION TO CONCRETE CRACK PROBLEMS

This study investigates crack propagation in concrete plates using the PFM–UEL framework implemented in Abaqus. Two types of specimens are considered: a square plate with a pre-existing notch (Fig. 4) and a rectangular plate with a pre-notched groove (Fig. 5). Boundary conditions and loading configurations vary among the cases to examine the effects of loading rate, direction, and mesh resolution on crack propagation.

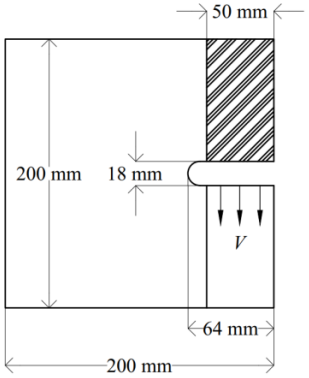

Fig. 4. Schematic of the concrete plate model with a pre-existing notch

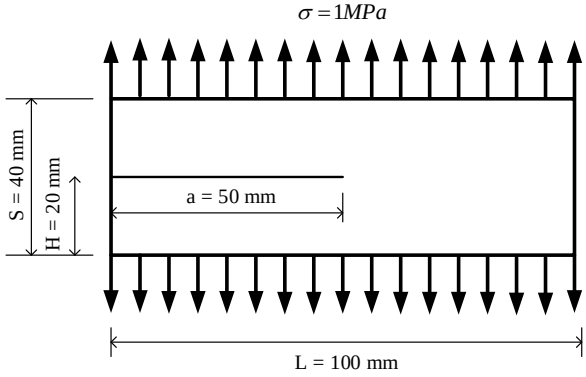

Fig. 5. Geometry and boundary conditions of the rectangular concrete plate with a pre-notched groove

The square plate (Fig. 4) has dimensions $200 \times 200 \times 50$ mm and contains a pre-existing notch of 64×18 mm. Concrete properties are assigned as: Young's modulus $E = 36$ GPa, Poisson's ratio $\nu = 0.18$, tensile strength $f_t = 3.80$ MPa, and fracture energy $G_c = 65\,\mathrm{J/m^2}$ and the mass density is taken as $\rho = 2400\,\mathrm{kg/m^3}$. For the rectangular plate (Fig. 5), a uniformly distributed tensile pressure of $P = 1$ MPa is applied on the top and bottom surfaces of the rectangular concrete plate promoting crack branching. Material properties are set as: $E = 32$ GPa, $\nu = 0.2$, $f_t = 3.80$ MPa, $G_c = 3\,\mathrm{J/m^2}$, with an assumed thickness of 0.002 m. The chosen values are consistent with typical ranges reported for normal-strength concrete in the literature (Bažant & Planas, 1998; Ožbolt et al., 2013).

3.1. Numerical results - square plate cases

Crack branching in concrete is influenced not only by material parameters and structural geometry but also by the loading rate. A higher loading rate increases the rate of energy release, which in turn accelerates crack tip motion. Although the fracture process zone in concrete modifies the critical threshold observed in brittle materials, rapid loading still promotes unstable propagation and branching. In other words, while the crack tip velocity is not directly prescribed, it is strongly driven by the applied loading rate. For this reason, the following parametric study examines how variations in loading rate affect crack propagation patterns and the onset of branching.

For the dynamic simulations in both cases, the regularization length scale was chosen as $\ell = 2 \times 10^{-3}$ m, and the uniform element size used in the fracture zone was $h = 10^{-3}$ m, satisfying the numerical stability criterion for the quadratic basis functions.

3.1.1. *Low-velocity case ($V = 1.4$ m/s)*

Under single-sided low-velocity loading, the pre-existing notch evolves into an almost straight crack spanning the depth of the plate (Fig. 6). The PFM–UEL simulation reproduces the principal features of the experimentally observed crack path reported by Ožbolt et al. (2013), including the dominant Mode I opening mechanism, the strong localization of elastic strain energy ahead of the crack tip, and the concentrated damage field that governs subsequent

crack advance. Contour plots of the phase-field variable ϕ and the elastic strain energy density confirm that the model captures the essential physics of quasi-static crack propagation.

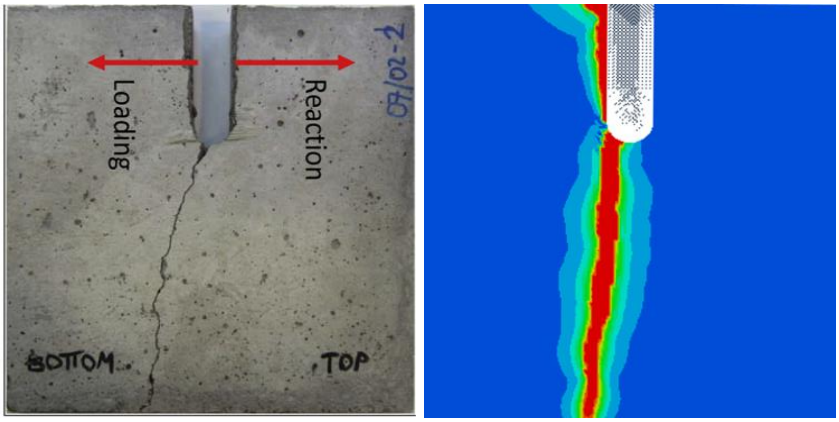

Fig. 6. Comparison of simulated and experimental crack propagation at $V = 1.4$ m/s

Minor differences appear in the detailed crack geometry: the experimental fracture path of Ožbolt et al. (2013) is slightly more tortuous and irregular, while the numerical simulation yields a smoother and more regular trajectory. These deviations arise from several factors: (i) the intrinsic regularization of the phase-field method, which spreads the crack over a finite length scale ℓ; (ii) the assumption of homogeneous concrete in the model, whereas real concrete contains aggregates and microcracks that perturb local stress fields; (iii) small variations in experimental boundary conditions or load alignment, which are idealized in the numerical framework; and (iv) numerical aspects such as mesh density, element type, and the calibration of ℓ and fracture energy G_c. Even under quasi-static conditions, rate effects or testing noise may also contribute to discrepancies. Overall, the comparison demonstrates that the proposed PFM–UEL model provides a reliable and physically consistent representation of straight-through crack propagation under low-velocity loading. While minor deviations remain, they can be rationalized as the combined result of modeling simplifications and unavoidable experimental variability.

3.1.2. *High-velocity case ($V = 3.3$ m/s, single-sided)*

Under a higher loading rate, the fracture response of the concrete plate changes markedly compared with the low-rate case in Fig. 6. As shown in Fig. 7, the crack initiated from the pre-existing notch no longer follows a single straight path but instead develops into multiple branches. The PFM–UEL simulation (left) reproduces this branching behavior reported by Ožbolt et al. (2013) (right), capturing both the onset and qualitative geometry of the bifurcation. Contours of the phase-field variable ϕ clearly illustrate the redistribution of damage and fracture energy into two distinct propagation paths, consistent with the experimentally observed deviation of cracks under dynamic conditions.

Some differences are nevertheless evident. In the simulation, the branches remain smoother and more symmetric, whereas in the experiment they appear more irregular and asymmetric due to the inherent heterogeneity of concrete, aggregate distribution, and microstructural randomness. The diffuse representation of the crack enforced by the phase-field length scale ℓ, together with the assumption of material homogeneity and idealized boundary conditions, tends to suppress the small perturbations and tortuous paths seen in real specimens. Taken together, these results confirm that the proposed PFM–UEL framework is sensitive to loading rate and capable of capturing the transition from straight-through crack propagation to branching instabilities. The model therefore provides reliable predictions of complex fracture patterns

under dynamic conditions, while also offering deeper insight into the redistribution of damage and fracture energy phenomena that are difficult to observe directly in laboratory experiments.

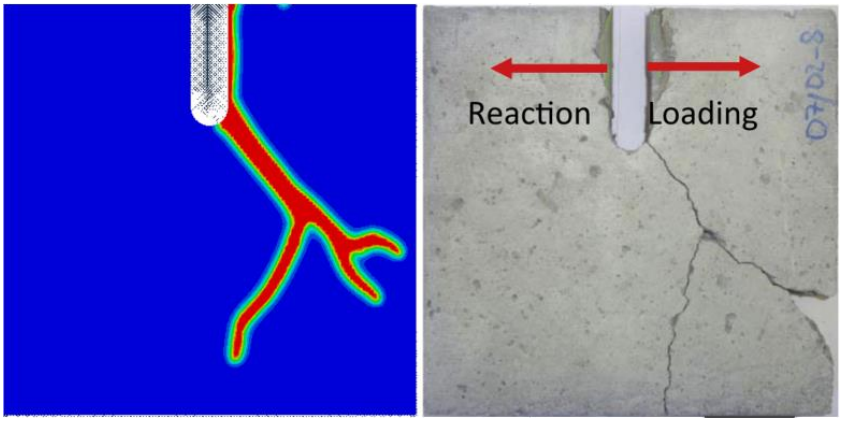

Fig. 7. Comparison of simulated and experimental crack propagation at $V = 3.3$ m/s

In addition to the physical observations of crack patterns under different loading rates, it is important to note that the numerical stability of the phase-field simulations is also influenced by the loading velocity. While the PFM–UEL framework successfully reproduces both single-crack propagation at low velocity ($V = 1.4$ m/s) and crack branching at higher velocity ($V = 3.3$ m/s), higher velocities result in rapid evolution of the phase-field variable ϕ, which can challenge solver convergence. In this study, the critical fracture energy $G_c = 65$ J/m^2 was maintained as a constant material parameter across all loading rates. This approach isolates the primary mechanism of branching, demonstrating that the transition from stable to branched cracks is governed by dynamic instability: when the input energy rate at $V = 3.3$ m/s exceeds the fixed dissipation capacity of a single crack tip, the PFM system is compelled to create multiple crack surfaces to dissipate the surplus kinetic energy.

Minor discrepancies in the detailed crack geometry between the simulated and experimental results are observed. These arise from the smeared crack representation inherent in the phase-field method, the assumption of homogeneous quasi-brittle concrete, and mesh discretization. Nevertheless, the PFM–UEL framework accurately captures the main fracture features, including the transition from single to branched cracks and the redistribution of damage and fracture energy, consistent with experimental observations.

It is well established that the conventional phase-field formulation tends to produce a smeared damage band wider than the actual fracture process zone, which may lead to an overestimation of the dissipated fracture energy, often approaching or even exceeding twice the theoretical value (Miehe et al., 2010; Pham et al., 2011). To evaluate this aspect in the present implementation, the total dissipated energy per unit thickness $E_{\text{diss-2D}}$ was computed by integrating the fracture energy contribution $(G_c\gamma(\phi, \nabla\phi))$ over the 2D domain Ω. For the simulated concrete plate, the theoretical fracture energy per unit thickness is estimated as: $E_{\text{th-2D}} = 14.625$ J/m. A mesh sensitivity analysis was performed to validate the energy calculation, with results presented in Fig. 8. This plot correctly demonstrates the physical behavior of the fracture process: the energy initiates at zero and increases smoothly as the crack propagates. This behavior is fully consistent with the findings of Borden et al. (2012). The plot also shows that the results from Mesh 1 and Mesh 3 are nearly identical, indicating that the solution is stable with respect to mesh refinement. However, the graph clearly shows that the trend of the simulated dissipated energy is significantly higher than the theoretical $E_{\text{th-2D}}$ value. This discrepancy, which persists even with finer meshes, raises an important academic point for discussion. We posit this can be explained by several factors: firstly, achieving perfect

energy convergence to the theoretical value is a known challenge in PFM. For instance, Borden et al. (2012) (in their Remark 4.5) also reported simulated energy values approaching twice the theoretical G_c even when using advanced adaptive mesh refinement (AMR) for an ideal brittle material. Secondly, the present study simulates quasi-brittle concrete, not an ideal brittle material. Concrete involves complex energy dissipation mechanisms (e.g., micro-cracking, aggregate friction) not fully captured by the single G_c parameter. Finally, the primary objective of this study is to develop a PFM-UEL framework suitable for generating large-scale datasets. This goal necessitates a computational trade-off: the model must be efficient on static meshes (which are computationally cheaper than AMR), thereby accepting the known PFM limitation of spurious energy dissipation. This energy convergence issue is identified as an important direction for future investigation.

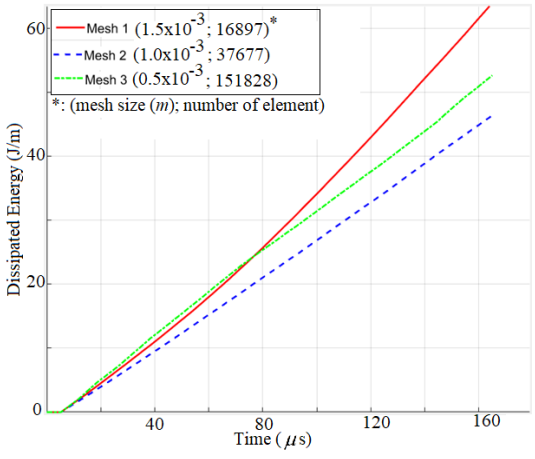

Fig. 8. Time evolution of cumulative dissipated energy per unit thickness (J/m) for the hight-velocity case (Fig. 6), showing results for three different mesh densities

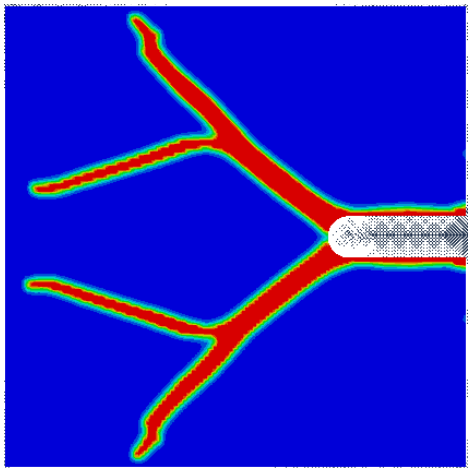

Fig. 9. Simulated crack propagation under symmetric tensile loading at $V = 3.3$ m/s

3.1.3. *Symmetric high-velocity case ($V = 3.3$ m/s, two-sided)*

When symmetric tensile loading is applied at a velocity of 3.3 m/s, the crack propagation pattern differs significantly from the single-sided cases. As shown in Fig. 9, the main crack emerging from the notch bifurcates into three primary branches, while the two outer branches further split into secondary cracks. The resulting morphology is highly symmetric and evenly distributed, reflecting the uniform stress field imposed by the boundary conditions. The phase-field contours ϕ clearly capture the simultaneous activation of multiple crack fronts and the redistribution of fracture energy into balanced propagation paths.

No direct experimental data are available for this loading configuration, but the numerical results provide valuable physical insights. In particular, the high degree of symmetry observed in the simulated crack network underscores the strong influence of loading configuration on fracture behavior: symmetric boundary conditions promote more uniform branching, in contrast to the asymmetric or irregular patterns seen under single-sided loading. This observation is consistent with theoretical expectations, since equal tensile forces on both sides reduce stress eccentricity and lead to simultaneous instability of multiple crack tips. These findings suggest that loading symmetry is a key factor governing the morphology of crack networks in quasi-brittle materials. The ability of the PFM–UEL framework to capture such patterns highlights its potential not only for simulating realistic fracture scenarios but also for generating systematic

datasets where the effect of load symmetry on crack branching can be explored in a controlled manner.

3.2. Rectangular plate with pre-notched groove

3.2.1. *Mesh sensitivity*

Figure 10 illustrates the influence of mesh density on the predicted crack paths in a rectangular plate with a pre-notched groove subjected to uniform tensile loading. When a fine mesh 0.25×10^{-3} is used, the simulation captures crack branching and subsequent directional changes with higher fidelity. The resulting cracks are smoother and more continuous, and secondary branching is reproduced with greater clarity. By contrast, the coarse mesh (0.5×10^{-3}) leads to a less accurate representation: the crack trajectory appears jagged and the details of branching are diminished, reducing the ability of the model to reflect the underlying fracture mechanisms.

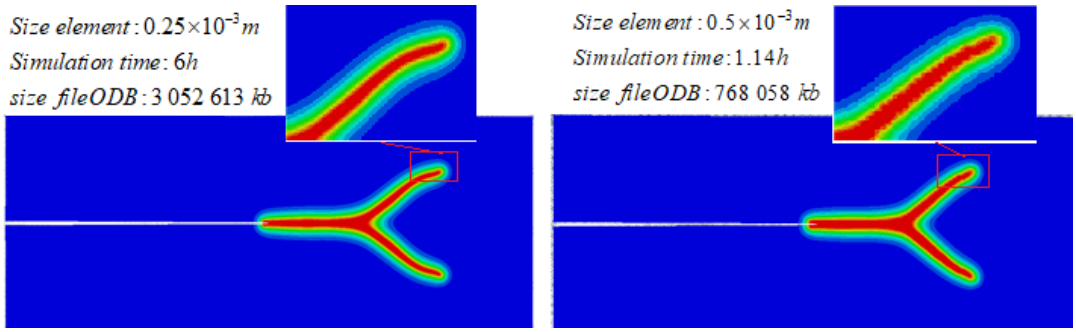

Fig. 10. Influence of mesh density on crack propagation

3.2.2. *Comparison with literature*

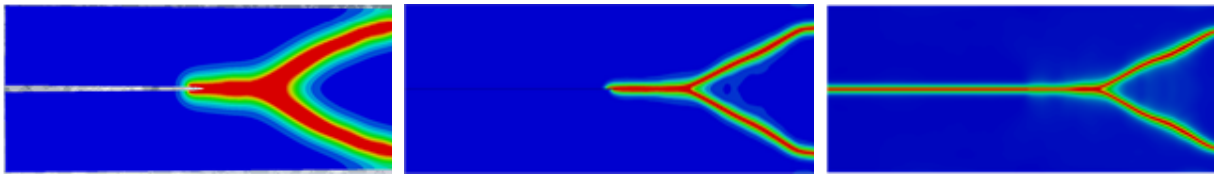

(a) Present study (b) Molnár et al. (2020) (c) Borden et al. (2012)

Fig. 11. Comparison of crack branching simulations using the PFM – UEL framework

This improvement in accuracy with mesh refinement, however, comes at a substantial computational cost. The fine mesh requires approximately six hours of computation and generates an output database of over 3 GB, whereas the coarse mesh reduces simulation time to little more than one hour and produces a file size of only 768 MB. Such differences highlight the trade-off between resolution and efficiency: while fine meshes are more reliable for detailed fracture analyses, coarse meshes may suffice for qualitative studies or parametric surveys where computational economy is critical.

These results emphasize the necessity of mesh sensitivity analysis when applying the PFM–UEL framework. Selecting an appropriate mesh size depends on the purpose of the study: fine discretization is essential when accurate branching paths or secondary cracks must be resolved, whereas coarser meshes can be adopted for preliminary exploration or large-scale dataset generation, provided that the associated reduction in accuracy is acknowledged.

Fig. 11 compares the present PFM–UEL simulation of crack branching with the benchmark works of Molnár et al. (2020) and Borden et al. (2012). In the present study, the main crack bifurcates into two symmetric branches at approximately 48 μs, accompanied by clear strain energy localization at the tips, reflecting stable and nearly ideal Mode-I propagation. Molnár et al. (2020) obtained similar branching but with smaller high-energy zones, whereas Borden et al. (2012) reported sharper crack contours and more concentrated energy fields, which can be attributed to the finer discretization and refined parameters adopted in their simulations.

The role of mesh and model parameters in these differences is summarized in Table 1. Compared with Molnár et al. (2020) and Borden et al. (2012), the present study employed a relatively coarser mesh $\left(0.5 \times 10^{-3}\right)$ and larger regularization length ($\ell = 2 \times 10^{-3}$ m), which smooths the crack profile and broadens the damage zone. By contrast, the finer element sizes and smaller time steps used in Borden et al. (2012) and Molnár et al. (2020) enabled sharper crack-tip resolution and more distinct branch morphology. Despite these differences, the overall branching pattern, symmetry, and underlying mechanism are reproduced consistently, confirming that the proposed PFM–UEL framework achieves good agreement with the literature.

Table 1. Mesh sensitivity parameters used in this study and comparison with previous works

	Present study	Molnár et al. (2020)	M. Borden et al. (2012)
Element size (m)	0.5×10^{-3}	0.125×10^{-3}	0.0625×10^{-3}
Crack width ℓ (m)	2×10^{-3}	0.5×10^{-3}	0.25×10^{-3}
Time step Δt (s)	10^{-7}	10^{-8}	2.5×10^{-8}

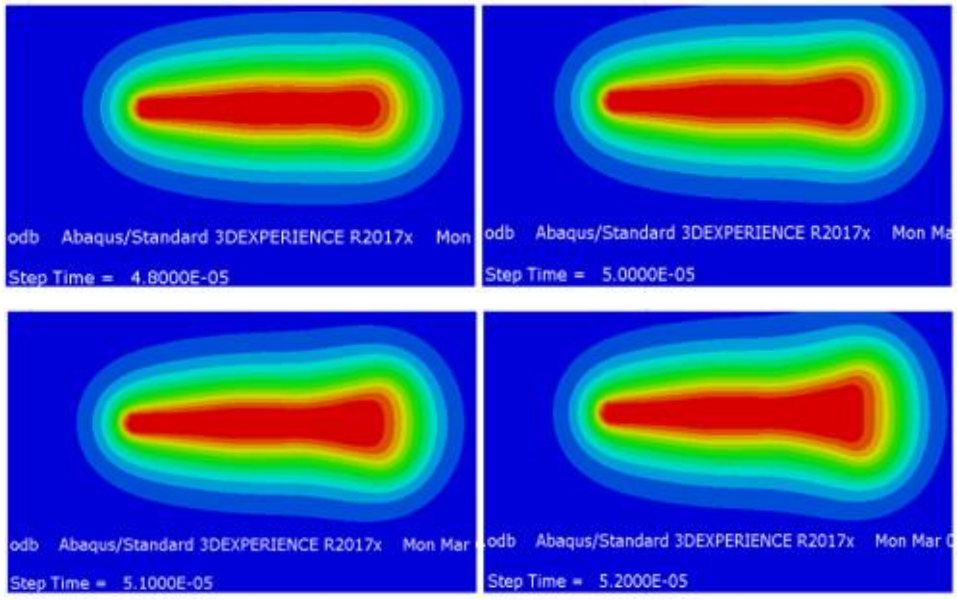

Fig. 12. Crack branching onset and subsequent propagation (step time)

To further substantiate this comparison, Fig. 12 illustrates the temporal evolution of branching in the present model. At $t = 4.8$ µs, a pronounced elliptical strain energy concentration appears at the notch tip. By $t = 5.0$ µs, the localization bifurcates into two lobes, and within (at $t = 5.2$ µs) a fully developed Y-shaped crack forms. This stepwise progression highlights the capability of the PFM–UEL framework to resolve not only the final branching morphology but also the onset timing with high temporal resolution.

Taken together, the comparisons in Figs. 11–12 and Table 1 demonstrate that the present PFM–UEL implementation reproduces the essential physics of crack branching in quasi-brittle materials. The model captures stable symmetry, realistic energy distribution, and branching onset consistent with theoretical and numerical benchmarks, while the observed minor discrepancies are largely attributable to mesh resolution, chosen length scale, and numerical settings.

4. CONCLUSION

This study presents an implementation of the PFM within the Abaqus–UEL framework to simulate crack initiation, propagation, and branching in concrete plates. Two benchmark problems—a square plate with an initial notch and a rectangular plate with a pre-notched groove—were analyzed to verify the framework. The numerical results successfully reproduced experimental and reference outcomes with good accuracy, capturing both straight and branched crack paths as well as the associated stress and energy distribution. These findings confirm that the PFM–UEL framework provides a robust and reliable tool for investigating complex fracture processes in quasi-brittle materials. The comparative analysis also highlighted the influence of mesh resolution, regularization length, and time increment on simulation accuracy. While a coarse mesh resulted in wider crack openings, the overall fracture patterns, crack initiation time, and propagation direction remained consistent. This demonstrates both the strengths and current limitations of the approach: although computational cost is still a challenge, the framework substantially reduces dependence on experiments and enables systematic studies under special or extreme loading conditions. Future work will focus on improving computational efficiency through adaptive meshing and parallel computing, and extending the framework to address more complex scenarios such as mixed-mode fracture, cyclic loading, and reinforced or large-scale concrete structures.

DECLARATION OF COMPETING INTEREST

The authors declare that they have no known competing financial interests or personal relationships that could have appeared to influence the work reported in this paper.

CREDIT AUTHOR STATEMENT

Vu Thi Thuy Anh: *Conceptualization, Methodology, Software, Supervision, Writing – review & editing*. Ha Chi Hieu: *Investigation, Validation, Data curation, Writing – original draft*. Phan Dang Huy: *Formal analysis, Visualization, Writing – original draft*.

FUNDING

This research received no specific grant from any funding agency in the public, commercial, or not-for-profit sectors.

REFERENCES

Abdulridha Lateef, H., Mahmood Laftah, R., & Abdulrazzaq Jasim, N. (2022). Investigation of crack propagation in plain concrete using phase-field model. *Materials Today: Proceedings*, *57*, 375–382. https://doi.org/10.1016/j.matpr.2021.12.146

Anh, V. T. T., Dinh, T. H., Giang, V. D., Le, C. H., Dat, N. D., & Duc, N. D. (2025). Concrete crack simulation and its machine learning application in propagation prediction. *Archives of Civil and Mechanical Engineering*, *25*(4). https://doi.org/10.1007/s43452-025-01229-z

Azinpour, E., Rzepa, S., Melzer, D., Reis, A., Džugan, J., & Cesar de Sa, J. M. A. (2023). Phase-field ductile fracture analysis of multi-materials and functionally graded composites through numerical and experimental methods. *Theoretical and Applied Fracture Mechanics*, *125*, 103906. https://doi.org/10.1016/j.tafmec.2023.103906

Bažant, Z. P., & Planas, J. (1998, March). *Fracture and size effect in concrete and other quasibrittle materials*. CRC Press. https://doi.org/10.1201/9780203756799

Borden, M. J., Verhoosel, C. V., Scott, M. A., Hughes, T. J., & Landis, C. M. (2012). A phase-field description of dynamic brittle fracture. *Computer Methods in Applied Mechanics and Engineering*, *217–220*, 77–95. https://doi.org/10.1016/j.cma.2012.01.008

Chung, N. T., Hai, H., & Hee, S. S. (2016). Dynamic analysis of high building with cracks in column subjected to earthquake loading. *American Journal of Civil Engineering*, *4*(5), 233–240. https://doi.org/10.11648/j.ajce.20160405.14

Dinh, T. H., Anh, V. T. T., Nguyen, T., Hieu Le, C., Trung, N. L., Duc, N. D., & Lin, C.-T. (2023). Towards vision-based concrete crack detection: Automatic simulation of real-world cracks. *IEEE Transactions on Instrumentation and Measurement*, *72*, 1–15. https://doi.org/10.1109/tim.2023.3328076

Dorduncu, M., Ren, H., Zhuang, X., Silling, S., Madenci, E., & Rabczuk, T. (2024). A review of peridynamic theory and nonlocal operators along with their computer implementations. *Computers & Structures*, *299*, 107395. https://doi.org/10.1016/j.compstruc.2024.107395

Duc, N. D., Duc, D. H., Thom, D. V., & Truong, T. D. (2018). A static buckling investigation of multi-cracked FGM plate based phase-field method coupling the new TSDT. *Acta Mechanica*. https://doi.org/10.1007/s00707-018-2256-6

Hai, L., Zhang, H., Wriggers, P., Huang, Y. J., Zhuang, X. Y., & Xu, S. L. (2024). 3D concrete fracture simulations using an explicit phase field model. *International Journal of Mechanical Sciences*, *265*, 108907. https://doi.org/10.1016/j.ijmecsci.2023.108907

Hang, P. T. (2015). *Frequency spectrum method in the study of vibration of cracked elastic beams under moving loads* [Doctoral dissertation, Hanoi].

Huong, N. T. V. (2016). *Bending vibration of prestressed beams under the action of moving bodies* [Doctoral dissertation, Hanoi].

Huong, N. T. V., Khang, N. V., & Dien, N. P. (2015). Dynamic response of a cracked and pre-stressed beam under the action of a moving body. *Journal of Science and Technology (Technical Universities)*, *106*, 58–62.

Khan, G., Ahmed, A., Liu, Y., Tafsirojjaman, T., Ahmad, A., & Iqbal, M. (2023). Phase field model for mixed mode fracture in concrete. *Engineering Fracture Mechanics*, *289*, 109439. https://doi.org/10.1016/j.engfracmech.2023.109439

Khiem, N., & Hang, P. (2017). Analysis and identification of multiple-cracked beam subjected to moving harmonic load. *Journal of Vibration and Control*, *24*(13), 2782–2801. https://doi.org/10.1177/1077546317694496

Li, X., & Xu, Y. (2022). Phase field modeling scheme with mesostructure for crack propagation in concrete composite. *International Journal of Solids and Structures*, *234–235*, 111259. https://doi.org/10.1016/j.ijsolstr.2021.111259

Miehe, C., Hofacker, M., & Welschinger, F. (2010). A phase field model for rate-independent crack propagation: Robust algorithmic implementation based on operator splits. *Computer Methods in Applied Mechanics and Engineering*, *199*(45–48), 2765–2778. https://doi.org/10.1016/j.cma.2010.04.011

Minh, P. P., Van Do, T., Duc, D. H., & Duc, N. D. (2018). The stability of cracked rectangular plate with variable thickness using phase field method. *Thin-Walled Structures*, *129*, 157–165. https://doi.org/10.1016/j.tws.2018.03.028

Molnár, G., Gravouil, A., Seghir, R., & Réthoré, J. (2020). An open-source Abaqus implementation of the phase-field method to study the effect of plasticity on the instantaneous fracture toughness in dynamic crack propagation. *Computer Methods in Applied Mechanics and Engineering*, *365*, 113004. https://doi.org/10.1016/j.cma.2020.113004

Nair, K. A., & Ghosh, S. (2023). Crack tip enhanced phase field model for crack evolution in crystalline Ti6Al from concurrent crystal plasticity FE-molecular dynamics simulations.

European Journal of Mechanics - A/Solids, *100*, 104983. https://doi.org/10.1016/j.euromechsol.2023.104983

Navidtehrani, Y., Betegón, C., & Martínez-Pañeda, E. (2021a). A unified Abaqus implementation of the phase field fracture method using only a user material subroutine. *Materials*, *14*(8), 1913. https://doi.org/10.3390/ma14081913

Navidtehrani, Y., Betegón, C., & Martínez-Pañeda, E. (2021b). A simple and robust Abaqus implementation of the phase field fracture method. *Applications in Engineering Science*, *6*, 100050. https://doi.org/10.1016/j.apples.2021.100050

Ožbolt, J., Bošnjak, J., & Sola, E. (2013). Dynamic fracture of concrete compact tension specimen: Experimental and numerical study. *International Journal of Solids and Structures*, *50*(25–26), 4270–4278. https://doi.org/10.1016/j.ijsolstr.2013.08.030

Pham, K., Amor, H., Marigo, J. J., & Maurini, C. (2011). Gradient damage models and their use to approximate brittle fracture. *International Journal of Damage Mechanics*, *20*(4), 618–652.

Reddy, S. S. K., Amirtham, R., & Reddy, J. N. (2021). Modeling fracture in brittle materials with inertia effects using the phase field method. *Mechanics of Advanced Materials and Structures*, *30*(1), 144–159. https://doi.org/10.1080/15376494.2021.2010289

Sun, Y., Edwards, M. G., Chen, B., & Li, C. (2021). A state-of-the-art review of crack branching. *Engineering Fracture Mechanics*, *257*, 108036. https://doi.org/10.1016/j.engfracmech.2021.108036

Tanné, E., Li, T., Bourdin, B., Marigo, J.-J., & Maurini, C. (2018). Crack nucleation in variational phase-field models of brittle fracture. *Journal of the Mechanics and Physics of Solids*, *110*, 80–99. https://doi.org/10.1016/j.jmps.2017.09.006

Truong, T. T., Lo, V. S., Nguyen, M. N., Nguyen, N. T., & Nguyen, D. K. (2021). Evaluation of fracture parameters in cracked plates using an extended meshfree method. *Engineering Fracture Mechanics*, *247*, 107671. https://doi.org/10.1016/j.engfracmech.2021.107671

Wang, C., Ping, X., & Wang, X. (2023). An adaptive finite element method for crack propagation based on a multifunctional super singular element. *International Journal of Mechanical Sciences*, *247*, 108191. https://doi.org/10.1016/j.ijmecsci.2023.108191

Wang, L.-X., Wen, L.-F., Tian, R., & Feng, C. (2024). Improved XFEM (IXFEM): Arbitrary multiple crack initiation, propagation and interaction analysis. *Computer Methods in Applied Mechanics and Engineering*, *421*, 116791. https://doi.org/10.1016/j.cma.2024.116791

Yu, X., Wang, R., Dong, C., Ji, J., & Zhen, X. (2023). 3D implementation of push-out test in ABAQUS using the phase-field method. *Journal of Mechanical Science and Technology*, *37*(4), 1731–1745. https://doi.org/10.1007/s12206-023-0314-z

Zhang, P., Cui, Y., Douglas, K., Song, C., & Russell, A. R. (2025). Phase field fracture modeling of cohesive-frictional materials like concrete and rock using the scaled boundary finite element method. *Computers and Geotechnics*, *180*, 107106. https://doi.org/10.1016/j.compgeo.2025.107106

Zhou, C., Hu, M., Xie, D., Wang, Y., & He, J. (2023). Finite element-based phase field simulation of complex branching crack propagation under different loads. *Mechanics of Advanced Materials and Structures*, *31*(18), 4269–4279. https://doi.org/10.1080/15376494.2023.2193184